Sharper and Faster "Nano Darts" Kill More Bacteria: A Study of Antibacterial Activity of Individually Dispersed Pristine Single-Walled Carbon Nanotube

Shaobin Liu, Li Wei, Lin Hao, Ning Fang, Matthew Wook Chang, Rong Xu, Yanhui Yang, and Yuan Chen*

School of Chemical and Biomedical Engineering, Nanyang Technological University, Singapore 637459

ABSTRACT To further our understanding on the antibacterial activity of single-walled carbon nanotubes (SWCNTs), high purity SWCNTs with average diameter of 0.83 nm and (7,5) chirality as dominate (*n*,*m*) structure were dispersed in a biocompatible surfactant solution. Ultraviolet—visible—near-infrared radiation absorption spectroscopy was employed to monitor the aggregation of SWCNTs. The results demonstrated that individually dispersed SWCNTs were more toxic than SWCNT aggregates toward bacteria (gram-negative *Escherichia coli*, *Pseudomonas aeruginosa*, and gram-positive *Staphylococcus aureus*, *Bacillus subtilis*). Individually dispersed SWCNTs can be visualized as numerous moving "nano darts" in the solution, constantly attacking the bacteria; thereby, degrading the bacterial cell integrity and causing the cell death. Controlled experimental results suggested that inhibiting cell growth and oxidative stress were not the major causes responsible for the death of cells. Furthermore, the detrimental effects of Co metal residues (up to 1 μg/mL) on SWCNT samples can be ruled out. Atomic force microscope study conducted in suspension proved that the death rates of bacteria were strongly correlated with their mechanical properties; soft cells were more vulnerable to SWCNT piercing. The antibacterial activity of SWCNTs can be remarkably improved by enhancing the SWCNT physical puncture on bacteria in the following ways: (1) dispersing SWCNTs individually to sharpen the nano darts; (2) increasing SWCNT concentration to raise the population density of nano darts; and (3) elevating the shaking speed of incubation to speed up the nano darts. This study elucidated several factors controlling the antibacterial activity of pristine SWCNTs and it provided an insight in developing strategies that can maximize the SWCNT application potentials while minimizing the health and environment risks.

KEYWORDS: single-walled carbon nanotube · antibacterial activity · aggregation · metal residue · atomic force microscope

INTRODUCTION

Since the discovery of carbon nanotubes (CNTs) in 1991,[1] a wide range of current and/or future applications of CNTs have been proposed owing to their amazing electronic, mechanical, and structural properties.[2,3] In recent years, the discovery of antibacterial activity[4] has triggered the exploration of environmental and human health applications of CNTs.[5] Robust and regenerative purification devices were fabricated using single-walled carbon nanotubes (SWCNTs) to remove the viral and bacterial pathogen.[6] Hybrid composites of CNTs with other components (*e.g.*, polymers or metal ions) can be effective in inhibiting microbial attachment and biofouling formation.[7,8] Biomimetic SWCNT coatings were applied to disinfect antimicrobial surfaces.[9] The advent of engineered CNTs in commercial and industrial applications raised concerns about the potential impacts of CNTs on human health and environmental safety.[10−13] From a scientific point of view, the best strategy for maximizing CNTs' application potentials while minimizing their risks, is to have a better insight in their toxicity mechanism. Based on such a mechanistic understanding, synthesis, purification, and functionalization procedures can be modified to avoid the specific features of CNTs that cause toxicity.[14]

Various, sometimes even contradictory, toxicity mechanisms have been proposed for CNTs including interruption of transmembrane electron transfer, disruption/penetration of the cell envelope, oxidation of cell components, and production of secondary products such as dissolved heavy metal ions or reactive oxygen species (ROS).[4,12,15−18] A major reason for the contradictory results obtained on CNTs may be ascribed to the heterogeneous nature of current available CNT samples due to the coexistence of many species including transition metal residues, nanosized catalyst supports, amorphous carbon, carbon nanoparticles, graphite, carbon fibers, multiwalled carbon nanotubes (MWCNTs) and SWCNTs. Toxicity of a CNT sample is dependent on its composition along with its geometry and surface functionalization. Several studies have suggested that well-functionalized, serum-stable CNTs are safe to animal cells, while raw CNTs or CNTs without functionalization show severe toxicity to animal or human cells at even

*Address correspondence to chenyuan@ntu.edu.sg.

Received for review June 6, 2009 and accepted November 3, 2009.

Published online November 6, 2009.
10.1021/nn901252r

moderate dosage.[19−24] The first direct evidence on the antibacterial activity of CNTs was reported by Kang *et al.*[4] By using high purity CNT samples with a low metal residue content dispersed in an aqueous saline solution, they suggested that the damage of membrane resulting from the direct contact with SWCNT aggregates was likely the mechanism leading to bacterial cell death.[4] They also found that SWCNTs were more toxic toward bacteria than large diameter MWCNTs, indicating the size (diameter) of CNTs was a key factor governing their antibacterial activity.[25] Moreover, short MWCNTs were more toxic when they were uncapped, debundled, and dispersed in solution.[26] Time dependence of antibacterial activity of CNTs has also been reported.[27] Recently, Arias and Yang have explored the effects of buffer selection, concentration, and CNT surface functional groups on the antibacterial activities of SWCNTs and MWCNTs.[28] These findings implied that an improved contact between CNTs and bacteria may lead to a superior antibacterial activity.

Because of strong $\pi-\pi$ interaction, CNTs usually bundle together in aqueous or organic solutions. One *in vitro* study has previously shown that the agglomeration affected MWCNT toxicity toward human cells.[29] Kang *et al.* showed that partially debundled MWCNTs of 4.1 μm (through functionalization in a mixture of H_2SO_4 and HNO_3) have higher bacterial toxicity than larger MWCNT bundles of 77 μm in diameter.[26] The aggregation kinetics of MWCNTs can be examined through time-resolved dynamic light scattering.[30] SWCNTs are much smaller in size with the average diameter of 1−2 nm compared to MWCNTs. It is reasonable to suspect that the aggregation of SWCNTs may also play a crucial role in controlling their antibacterial activities. However, due to the difficulty in debundling SWCNTs and characterizing their aggregation state (note that light scattering techniques may have problems in determining the aggregation due to the tiny dimension of SWCNT bundles), to the best of our knowledge, previous studies have utilized either suspended or deposited SWCNT aggregates in the antibacterial activity evaluation other than individually dispersed SWCNTs. On the other hand, the bioavailability of metal residues (*e.g.*, Fe[15] and Ni[31]) on CNT samples was found to exist at toxicologically significant concentrations despite its apparent encapsulation by carbon, although a recent study showed no correlation between residual metal content and toxicity.[26]

We have previously developed a novel catalyst, MCM-41 (a siliceous mesopores molecular sieve) supported controllable subnanometer scale Co metal clusters (Co-MCM-41). It produces SWCNTs with a narrow diameter distribution containing *ca.* 20 different (*n,m*) nanotubes.[32−34] More recently, a facile centrifugation-based purification protocol has been developed to purify SWCNTs from Co-MCM-41 catalyst.[35] Purified SWCNTs have a purity index of 0.268, approaching the previously estimated value (~0.325) for analytically pure SWCNTs.[36] By tuning the centrifugation forces, SWCNT samples containing different amounts of metal residues (ranging between 19.28 and 0.17 atom %) can be easily obtained.[35] Furthermore, surfactant molecules adsorbed on SWCNT can be eliminated by heating the SWCNT in air after removal of metal residues. This allows redispersing "naked" SWCNTs in biocompatible surfactants.

In this study, a comprehensive study on the antibacterial activity of pristine SWCNTs was reported. Both gram-negative bacteria (*Escherichia coli* and *Pseudomonas aeruginosa*) and gram-positive bacteria (*Staphylococcus aureus* and *Bacillus subtilis*) were selected as bacterial models. The motivation of this study was to elucidate the effect of aggregation and metal residue contents on the antibacterial activity of SWCNTs, and subsequently to prove or disprove some key factors which may influence the SWCNT antibacterial activity. The different aggregation states of SWCNTs were achieved by dispersing them in saline solution, Tween-20, and sodium cholate (SC). Results showed that individually dispersed SWCNTs in biocompatible surfactant solutions possessed stronger antibacterial activity than SWCNT aggregates. The cell death was caused by physical puncture of SWCNTs, rather than inhibiting cell growth or oxidative stress. We also proved that the antimicrobial properties of SWCNTs were independent of cobalt residues remaining in SWCNT samples. Investigation on the mechanical properties of bacterial cell surface by atomic force microscope (AFM) in aqueous solution suggested that bacteria with softer surfaces were more vulnerable to SWCNT piercing which resulted in membrane damage leading to higher cell death rate.

RESULTS AND DISCUSSION

Individually Dispersed Pristine SWCNT. For many toxicity or antibacterial activity studies on nanomaterials, the lack of a comprehensive characterization on nanomaterials complicates the interpretation of experimental results. In this study, we took the advantages of controlled SWCNT synthesis[32−34] and facile purification procedure[35] and performed a detailed characterization on the tube samples. In the Supporting Information, Figure S1 shows the SWCNT characterization results obtained by various techniques. Raman spectra in Figure S1A display strong radial breathing mode (RBM) peaks and G bands along with very weak D bands, suggesting that a minimum amount of amorphous carbon and few defects or functional groups exist on the tube samples. It also demonstrates that our centrifugation-based purification protocol[35] does not alter the physicochemical properties of pristine SWCNTs. Figure S1B shows a single peak at 420 °C on the differential thermogravimetric analysis (DTG) curve in thermogravimetric analysis (TGA), confirming the absence of amorphous or graphitic nanoparticles byproducts exist.

Photoluminescence (PL) intensity map in Figure S1C readily shows that individually dispersed SWCNT samples have a narrow (*n,m*) distribution with an average tube diameter of 0.83 nm, the most abundant (*n,m*) species is (7,5) which accounts for 45% of semiconducting tubes. When diluted SWCNT dispersions were dried on a mica surface, AFM image in Figure S1D shows that tubes form small bundles. The length of individual tubes is about 1 μm. SWCNT films were also formed by filtering the SWCNT dispersions on a membrane and inspected by scanning electron microscope (SEM). Larger tube bundles can be observed in the SEM image from Figure S1E. Transmission electron microscope (TEM) image from Figure S1F reveals that SWCNT bundles have diameters ranging from 5 to 50 nm in the deposited films. SEM and TEM results also confirm the successful removal of carbon impurities and metal residues.

Pristine SWCNTs would aggregate to form bundle structures other than individually dispersed tubes in aqueous solvent because of the π−π interaction. Ultraviolet−visible−near-infrared radiation (UV−vis−NIR) absorption spectroscopy is a convenient tool to monitor the bundle formation in SWCNT dispersions. Charge transfers among tubes in a SWCNT bundle can quench and broaden their absorption peaks. We propose that this technique should be applied in SWCNT toxicity studies for monitoring the aggregation state of SWCNT samples. Simple sonication in saline solution or buffers cannot produce stable individually dispersed pristine SWCNTs. A soluble SWCNT sample can be obtained by either covalent functionalization or noncovalent dispersion of SWCNT. In this study, SWCNTs were dispersed by biocompatible surfactants (Tween-20 and SC) because the covalent functionalization introduces new functional groups to SWCNTs which may alter their toxicity and antibacterial properties.[28] Figure 1A shows that clear SWCNT dispersions can be obtained right after sonication in three different solutions (Tween-20, SC, and conventional saline as a comparison). Both Tween-20 and SC are effective surfactants for solubilizing SWCNTs[37−40] because no changes were observed for SWCNT dispersions after standing still for 2 h. On the other hand, SWCNTs dispersed in saline solution would aggregate, and carbon residues started depositing out of solution once the sonication was stopped. The SWCNT dispersions after the sonication were further characterized using UV−vis−NIR spectroscopy, as shown in Figure 1B. The SWCNT dispersions in Tween-20 and SC after 2 h preserve clear and sharp absorption peaks from both E_{11} and E_{22} transitions of SWCNTs, suggesting that most of tubes are individually dispersed in these two solutions. In the contrast, absorption peaks from SWCNTs originally dispersed in saline solution completely disappear, implying that SWCNT bundles are dominant.

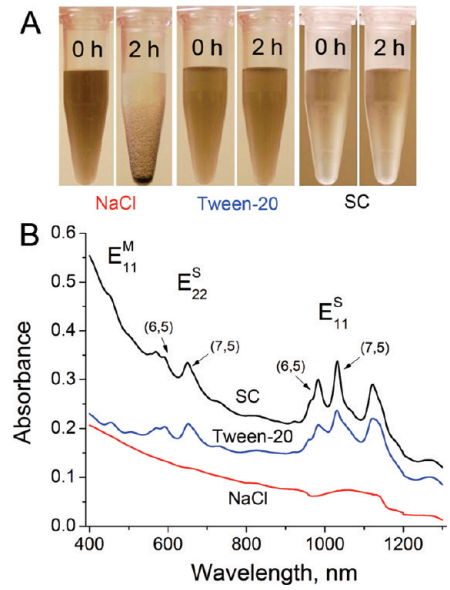

Figure 1. (A) SWCNTs dispersed in saline solution (NaCl, 0.9 wt %), Tween-20 saline solution (0.1 wt % and NaCl 0.9 wt %), and SC (1 wt %); right after sonication (0 h) and standing still for 2 h (2 h). (B) UV−vis−NIR spectra of SWCNT dispersions after standing still for 2 h. The concentration of measured SWCNT dispersions is at 20−30 μg/mL.

Biocompatibility of Surfactant Solutions. Although the surfactants have been demonstrated to be able to enhance of the dispersion of SWCNTs, the biocompatibility of surfactant solutions has to be studied first because they may also complicate the SWCNT antibacterial study due to their own antibacterial activities.[41] Gram-negative bacteria (*E. coli* and *P. aeruginosa*) and gram-positive bacteria (*B. subtilis* and *S. aureus*) were incubated for 2 h with the following solutions: 0.9 wt % NaCl (control), 0.1 wt % Tween-20 and 0.9 wt % NaCl mixture, and 1 wt % SC solutions. The colony forming count method was adopted to determine the survival rates of bacteria. Figure 2A shows that the survival rates of *E. coli* are 88.6 ± 1.7% and 86.9 ± 1.0% in the control and Tween-20 saline solution, respectively, and those of *P. aeruginosa* are 88.0 ± 2.0% and 88.5 ± 3.6%. The survival rates in these two solutions are 87.7 ± 1.8% and 87.9 ± 3.2% for *B. subtilis*, and 90.0 ± 3.6% and 90.4 ± 2.2% for *S. aureus*. These results show that the Tween-20 saline solution has no significant impacts on the viability of both gram-negative bacteria and gram-positive bacteria, which is similar to a previous study[39] claiming that Tween-80 can be used to disperse SWCNTs for toxicity studies. On the other hand, SC solution demonstrated a strong antibacterial activity. The survival rates of *E. coli*, *P. aeruginosa*, *B. subtilis,* and *S. aureus* are 46.5 ± 2.5%, 41.1 ± 3.9%, 42.7 ± 3.6%, and 50.8 ± 2.8%, respectively. Several previous studies have also reported that the adsorption of SC on cell membrane may change the membrane permeability due to the structural changes of cell membranes.[42,43]

Antibacterial Activity of SWCNTs Dispersed in Solutions. The antibacterial activities of SWCNTs dispersed in different

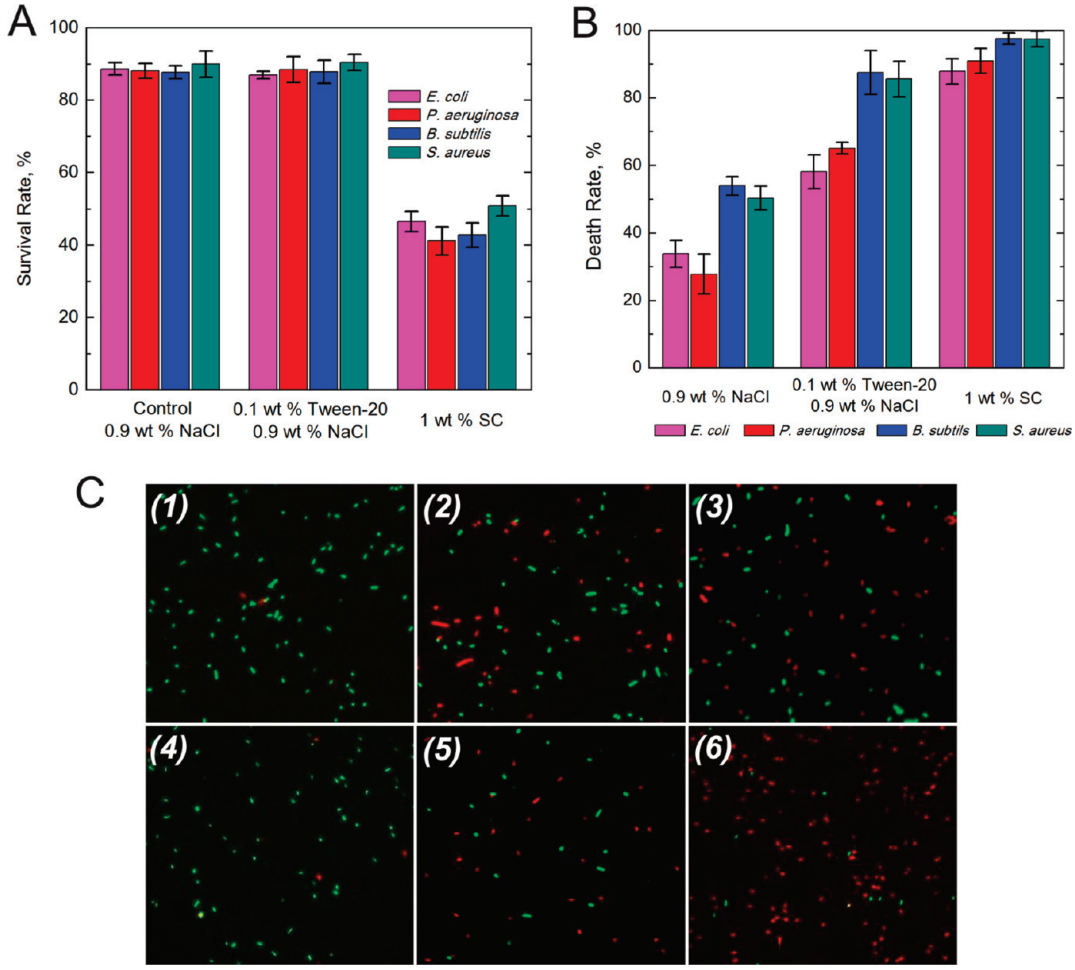

Figure 2. (A) Cell viability measurements after incubation with different surfactant solutions. Surfactant solutions (10 mL) were incubated with 1 mL of different bacterial suspensions (10^6-10^7 cfu/mL) for 2 h at 37 °C (30 °C for *B. subtilis*), respectively. Survival rates were obtained by the colony forming count method. Error bars represent the standard deviation. (B) Death rate of bacteria after incubation with SWCNTs dispersed in three different solutions. A 10 mL portion of SWCNT dispersion (5 μg/mL) was incubated with 1 mL of different bacterial suspensions (10^6-10^7 cfu/mL) for 2 h at 250 rpm shaking speeds, and at 37 or 30 °C. (C) Fluorescence microscope images of bacteria: (1) *E. coli* in 0.9 wt % NaCl control solution without SWCNTs; (2) *E. coli* after incubation with SWCNTs dispersed in saline solution; (3) *E. coli* after incubation with SWCNTs dispersed in the mixture of 0.1 wt % Tween-20 and 0.9 wt % NaCl; (4) *B. subtilis* in control solution without SWCNTs; (5) *B. subtilis* after incubation with SWCNTs dispersed in saline solution; (6) *B. subtilis* after incubation with SWCNT dispersion in the Tween-20 saline solution.

solutions were evaluated first by a colony forming count method. Figure 2B shows that SWCNTs dispersed in Tween-20 saline solutions exhibit high antibacterial activities; they kill 58.1 ± 5.0% of *E. coli*, 65.1 ± 1.8% of *P. aeruginosa*, 87.5 ± 6.5% of *B. subtilis,* and 85.6 ± 5.3% of *S. aureus*. As control experimental results, SWCNTs dispersed in saline solutions only kill 33.8 ± 4.0% of *E. coli*, 27.7 ± 5.9% of *P. aeruginosa*, 53.9 ± 2.8% of *B. subtilis*, and 50.3 ± 3.5% of *S. aureus*. Both saline and Tween-20 solutions show very similar biocompatibility as illustrated in Figure 2A. Therefore, the remarkably different antibacterial activities presented in Figure 2B can be attributed to the distinct SWCNT aggregation states in these two solutions, as evidenced in Figure 1B, because numerous SWCNT aggregates were observed during the incubation with bacteria in saline solutions but not in Tween-20 saline solutions. We conclude that SC is not a suitable surfactant for investigating the antibacterial activity of SWCNT samples because of the complication originating from the inherent high antibacterial activity of SC itself, although Figure 2B suggests that SWCNTs dispersed in SC solutions possess very high antibacterial activities. Therefore, the following assays in this study will focus on SWCNTs dispersed in Tween-20 saline solutions.

To verify the reliability of the colony forming count method in this particular study, *E. coli* and *B. subtilis* were chosen as models to further examine their death rates after incubation with SWCNT dispersions by a LIVE/DEAD BacLight bacterial viability kit (Invitrogen, USA). Similar fluorescence dye methods have been applied in previous CNT toxicity studies.[4,26] Membrane-permeant SYTO 9 labels live bacteria with green fluorescence, and membrane-impermeant propidium iodide (PI) labels membrane-compromised bacteria with red fluorescence. The results in Figure 2C show that the

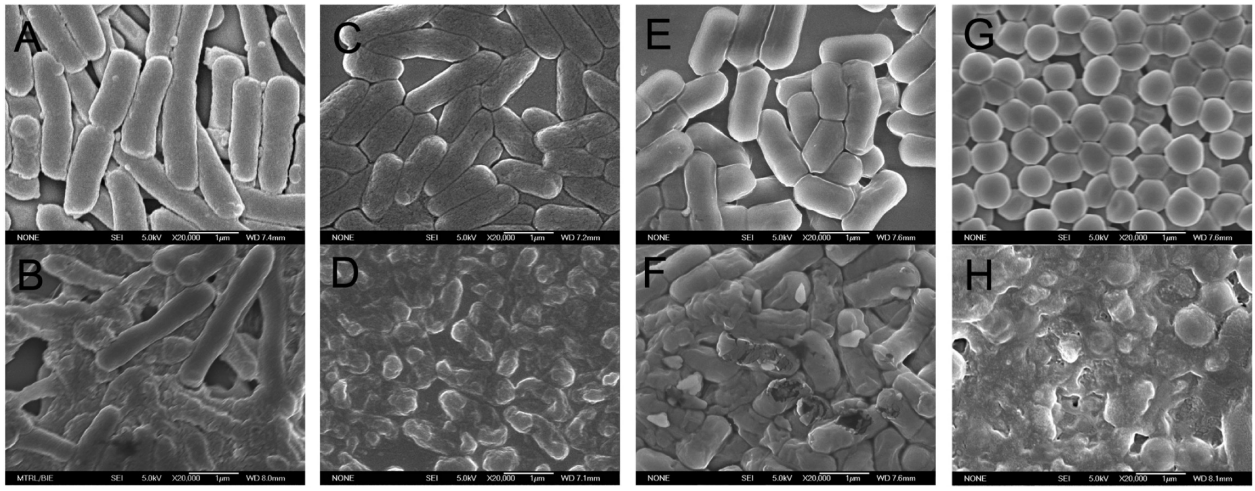

Figure 3. SEM images of (A) *E. coli* after incubation with saline solution for 2 h without SWCNTs, (B) *E. coli* after incubation with SWCNTs dispersed in the Tween-20 saline solution (0.1 wt % Tween-20 and 0.9 wt % NaCl) for 2 h, (C) *P. aeruginosa* without SWCNTs, (D) *P. aeruginosa* with SWCNTs, (E) *B. subtilis* without SWCNTs, (F) *B. subtilis* with SWCNTs, (G) *S. aureus* without SWCNTs, (H) *S. aureus* with SWCNTs.

fluorescence-based assay is in good agreement with the results obtained by the colony forming count method. A brief summary can be drawn from these antibacterial activity results: (1) individually dispersed SWCNTs in Tween-20 saline solutions possess higher antibacterial activities compared to SWCNT aggregates. (2) SWCNT dispersions show higher antibacterial activities toward gram-positive bacteria than gram-negative bacteria.

Destruction of Bacterial Membrane. Two intriguing questions arise from our antibacterial activity results: (1) why individually dispersed SWCNTs have higher antibacterial activities than SWCNT aggregates and (2) why gram-positive bacteria are more vulnerable to SWCNTs than gram-negative bacteria. To answer these two questions, we have to first know how SWCNTs interact with bacteria. Several previous studies[4,25−27] have proposed that the antibacterial activity of SWCNTs is associated with the damage of cell membrane upon the direct contact between SWCNT aggregates and bacteria. If the bacterial membrane is compromised, the release of cytoplasmaic constituents, such as DNA and RNA can be monitored by their strong UV absorption at 260 nm.[44] The Supporting Information, Figure S2 shows our UV−vis study on the release of 260 nm absorbing materials after we incubated the bacteria with SWCNTs. The optical density (OD) ratio of a bacterium suspension with SWCNTs to a bacterium suspension without SWCNTs is plotted. This ratio shows a remarkable increment by a factor of 3.2 times after bacteria interacting with SWCNTs. Two additional features are observed in Figure S2: (1) the OD_{260nm} ratios of *E. coli* and *B. subtilis* are 1.5 −1.6 times in Tween-20 saline solutions compared to in saline solutions. (2) The OD_{260nm} ratios of *B. subtilis* are about 30% higher than those of *E. coli* suspensions. The results from this absorption study at 260 nm are in agreement with cell viability measurements, suggesting that the reflux of DNA and RNA correlates to the bacterial mortality. It also implys that the bacterium death is directly associated with the damage of bacterial membrane.

The damage of bacterial membrane was further illustrated by a SEM study shown in Figure 3. *E. coli*, *P. aeruginosa*, *B. subtilis*, and *S. aureus* in saline solutions without SWCNTs maintain their integrity of the membrane structure after 2 h incubation (Figure 3A,C,E,G). In contrast, this cellular integrity disappears when the cells were incubated with SWCNTs dispersed in Tween-20 saline solutions for 2 h (Figure 3B,D, F,H). Similar SEM images of various bacteria after incubation with CNTs have been reported before.[4,25−28] However, it should be noted that individually dispersed SWCNTs were employed in this antibacterial activity study which is significantly different from the previous SEM studies in the presence of many CNT bundles. The reason why only few SWCNTs are visualized in our SEM images may be because individually dispersed SWCNTs that are 1−2 nm in diameter are difficult to observe in SEM.

The Cause of Bacterial Membrane Destruction. Previous studies have attributed the antibacterial activity of SWCNTs to the physical puncture of SWCNT aggregates, resulting in the physical damages of the outer membrane of the cells.[4,26] Findings in the present study by SEM and UV absorption at 260 nm and SEM support such an argument. We name the individually dispersed SWCNTs as "nano darts", which degrade the bacterial cell integrity by attacking them in the solution. However, other factors may also contribute to the bacterial membrane destruction, such as inhibiting cell growth, oxidative stress, and metal residues; controlled experiments were carried out to prove or disprove their roles on the antibacterial activity of SWCNTs.

The bacteria used in this study are viable and capable of growth. Thus, other than the direct physical puncture, SWCNTs may also cause the bacterial death by inhibiting the cell growth during the 2 h incubation.

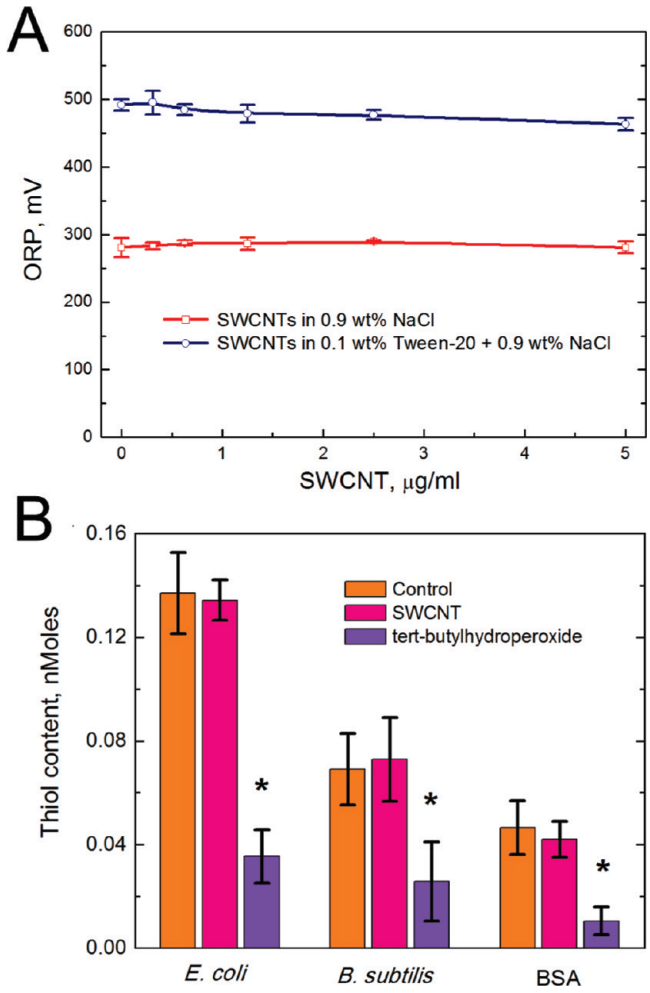

Figure 4. (A) Oxidation−reduction potential of SWCNTs dispersed in saline solutions and Tween-20 saline solutions. (B) Protein oxidation in cell extracts of *E. coli* and *B. subtilis*, and BSA by measuring thiol concentration; 10 mL of SWCNTs (5 μg/mL, dispersed in the Tween-20 saline solution) were incubated with 1 mL of cell suspensions (10^6 to 10^7 cfu/mL). Cell extracts containing about 2.5 μg of proteins determined by a Pierce BCA protein assay kit were used for thiol assays, while 3 μg of BSA (diluted from 2 mg/mL concentrated solution) was used for cell-free assays.

To evaluate this possibility, the cell growth rates in Luria−Bertani (LB) broth and the Tween-20 saline solution were first compared. In the Supporting Information, Figure S3A shows that both *E. coli* and *B. subtilis* cells can grow in LB broth, while no observable cell growth in the Tween-20 solution can be discerned. The survival rate of bacteria (*E. coli* and *B. subtilis*) is about 88% after incubation with the Tween-20 saline solution for 2 h (Figure 2A), indicating that most cells can survive without growth in the 2 h incubation period used in our SWCNT antibacterial activity assays. We also investigated the effect of a typical bacterial static agent on the cells while they were exposed to SWCNTs. Sulfadiazine is a bacteriotatic agent at low concentration.[45,46] It can interfere with bacterial synthesis of folic acid needed by cell growth.[47] Sulfadiazine can inhibit growth and reproduction of bacteria without killing them. The death rate of bacteria during their incubation with SWCNTs would decrease in the presence of such a bacterial static agent in SWCNT dispersions if SWCNTs can kill bacteria by inhibiting cell growth. We compared the death rate of bacteria after incubation of SWCNT dispersions with and without the presence of sulfadiazine, as well as after incubation with sulfadiazine alone. Figure S3B of the Supporting Information shows that bacteria incubated with sulfadiazine in the absence of SWCNTs had a very low death rate (<10%). The remarkably high death rates of bacteria after incubation with SWCNTs and sulfadiazine are the same as incubating the bacteria using SWCNT alone. These control results indicate that inhibiting cell growth by SWCNTs is not a major cause responsible for the death of cells in this study.

Another possible mechanism for SWCNT antibacterial activity is the oxidative stress. A SWCNT can be sometimes considered as an extended fullerene (C_{60}). They are both made of pure carbon, and their diameters are at a similar size. Because the oxidative stress was identified as a major mechanism for C_{60} toxicity, it is reasonable to suspect that oxidative stress can be one of the major mechanisms for SWCNT antibacterial activity. Lyon *et al*. have shown that fullerene exerts reactive oxygen species (ROS) independent oxidative stress on bacteria with the evidence of protein oxidation, changes in cell membrane potential, and interruption of cellular respiration.[48,49] Moreover, *E. coil* expresses high content of stress-related gene products after incubation with CNTs, implying that the antibacterial activities of CNTs may be partially contributed by oxidative stress.[25] We modified those two assays applied in the previous C_{60} studies[48,49] to further investigate the possibility of SWCNT induced oxidative stress. The oxidation−reduction potentials (ORP) of SWCNT suspensions were measured using an ORP tester (Oakton Instruments, ORPTestr 10). A significant increase in the ORP values is expected when the SWCNT concentration is increased, if SWCNT is a strong oxidant. The ORP of SWCNT dispersions at various concentrations in saline solutions and Tween-20 saline solutions was depicted in Figure 4A. Surprisingly, no increase of ORP values was observed with the increase of SWCNT concentration, suggesting SWCNT is not a strong oxidant in our tests, which is completely different from the results obtained on C_{60} dispersed in water.[49] Following the same protocol applied to the previous C_{60} study,[48] a thiol and sulfide quantitation kit (Molecular Probes, Invitrogen) was also utilized to measure the loss of thiol groups (−SH) on the proteins upon exposing cells to SWCNTs. Thiol groups exist on both bacterial membrane proteins and cytoplasmic proteins. Upon exposure to ROS or other oxidants, thiols can be oxidized. The level of thiols in proteins is an indication of oxidative damage to cellular components. The SWCNT oxidation of proteins both inside and outside of cell membranes was assessed. As shown in Figure 4B, the cell extracts obtained from *E. coli* and *B. sub-*

tilis after inculcating with SWCNT dispersions were tested. The *E. coli* extract has 0.137 ± 0.016 nmoles of thiol in the control sample and 0.134 ± 0.008 nmoles in the SWCNT-exposed sample. Similarly, the *B. subtilis* extract has 0.069 ± 0.014 and 0.073 ± 0.016 nmoles in the control sample and in the SWCNT-exposed sample, respectively. The similar thiol concentrations for both bacteria indicate that no thiol oxidation occurs after exposing to SWCNTs under anoxic conditions. Comparing with the previous C_{60} results,[48] we suggest that SWCNTs remain primarily outside the cell and cannot easily enter the cell membrane to oxidize cytoplasmic proteins. Therefore, if SWCNTs can apply a strong oxidative stress on the bacteria, the oxidation would only primarily occur at the membrane interface. Along this line, we examined the oxidation of a free protein bovine serum albumin (BSA) by SWCNTs in a cell-free assay. Figure 4B shows that the thiol concentrations are 0.047 ± 0.010 and 0.042 ± 0.007 nmoles in the control sample and in the BSA and SWCNT mixture, respectively, which is fairly close to the theoretically calculated 0.045 nmoles (3 μg of BSA) of the thiol in this assay. No oxidization of BSA by SWCNTs was observed, suggesting that the proteins on the bacterial membrane are unlikely to be oxidized by SWCNTs. Although we cannot exclude the possibility that oxidative stress induced by SWCNTs may partially contribute to SWCNT antibacterial activity, it appears not to play a major role in this study. Furthermore, it is reasonable to suggest that SWCNTs are remarkably different from C_{60} in terms of the toxicity owing to the significant difference in the physical and chemical properties between these two carbon materials. The large length-to-diameter aspect ratio of SWCNTs makes them behave more like nano darts.

Influence of Cobalt Residues on SWCNTs. The bioavailability of metal residues on CNT samples sometimes complicates CNT toxicity studies.[15,31] In this study, we are capable of looking into this issue in a systematic way because the advantages of our synthesis and purification methods of SWCNTs are obvious: only monometallic Co was employed as the catalysts for growing SWCNTs, and centrifugation-based purification allows us to obtain pristine SWCNTs containing a controllable amount of Co metal residues.[35] The antibacterial activities of SWCNT samples obtained after centrifugation at different speeds were studied on both *E. coli* and *B. subtilis*, and the results are shown in Figure 5. The cobalt content ranging from 19.28 to 0.17 atom % was determined by SEM−energy dispersive spectroscopy (EDS). The cobalt residue does not display impact on the SWCNT antibacterial activity in this study because no significant differences on their antibacterial activity were observed among different SWCNT samples. Furthermore, the UV−vis study on the release of 260 nm absorbing materials was performed. As shown in Figure S4 in the Supporting Information, various SWCNT

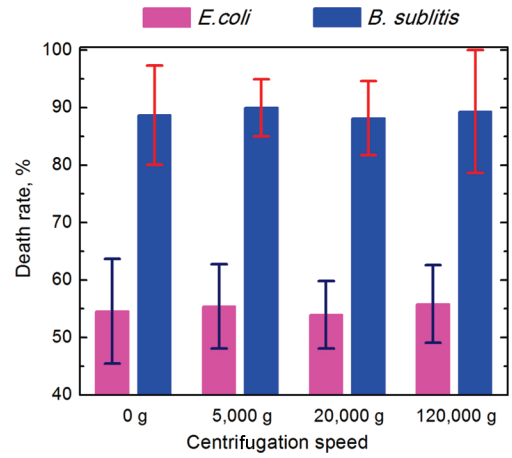

Figure 5. Antibacterial activities of SWCNTs obtained after centrifugation at different forces. SEM-EDS results indicated that SWCNT samples marked as "0*g*" contained 19.28 atom % Co and samples marked as "120000*g*" contained 0.17 atom %. A 10 mL portion of SWCNT dispersion (5 μg /mL) was incubated with 1 mL of bacterial suspensions (10^6−10^7 cfu/mL) for 2 h at 250 rpm shaking speeds and at 37 or 30 °C.

samples show similar OD_{260nm} ratios. This negligible effect of cobalt residue may be because a low SWCNT concentration (5 μg/mL) was used. It is converted into a maximum Co concentration at approximate 1 μg/mL (for SWCNT samples containing 19.28 atom % Co). We also tested the antibacterial activity of saline solution containing different amounts of $Co(NO_3)_2$. The increase of bacterial death rate can be observed only when the Co^{2+} concentration is 40 μg/mL or above, which is way higher than the Co residue left in SWCNT dispersions in this antibacterial activity study.

AFM Study of Bacteria. In this antibacterial activity study, significant differences were observed on the death rates of *E. coli*, *P. aeruginosa*, *B. subtilis*, and *S. aureus*. From a solely mechanical interaction perspective, the collision between SWCNTs and bacteria should be sensitive to mechanical properties of bacterial surfaces. We applied AFM to investigate the cell mechanical properties in an attempt to reveal their correlation with the cell death rates. AFM is a powerful imaging tool capable of achieving high resolution imaging of cells as well as the mechanical properties of surfaces. Initial AFM measurement was carried out in a dry environment because it is convenient to obtain high resolution images. In the Supporting Information, Figure S5 panels A and B are AFM height profiles of dried *E. coli* and *B. subtilis* on glass slides. Before interacting with SWCNTs, both bacteria demonstrated smooth cell surfaces consistent with observations in SEM. Mechanical properties of cell surfaces can be investigated by relating the applied force to the indentation depth as the AFM tip is pushed onto a soft sample.[50] After obtaining AFM images, AFM tips were pushed onto different locations on bacterial surfaces. The force applied was 3 nN, which did not damage the bacteria because identical force−distance

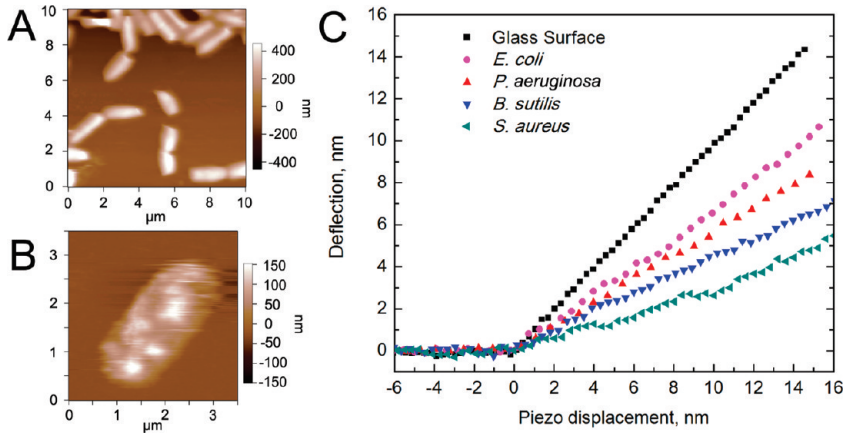

Figure 6. Typical AFM height profiles of (A) *B. subtilis* and (B) *E. coli* obtained in saline solution. Once images were taken, AFM tips were pushed onto different locations on bacterial surfaces to obtain the force−distance curve. (C) Typical force−distance curves obtained on glass surface, *E. coli*, *P. aeruginosa*, *B. subtilis*, and *S. aureus*.

curves can be obtained on the same location at bacterial surfaces. Figure S3C shows the typical force−distance curves obtained on glass and two bacterial surfaces. The cantilever deflection resulting from the approach of the AFM tip was monitored as a function of the piezo movement.[51] For a hard surface, the slope of the linear portion of the force−distance curve should be 1 because the AFM tip cannot induce any indentation on the hard surface. The slopes of the force−distance curves obtained on bacterial surfaces are less than 1 because of the deformation of cell membranes under force. No significant differences are observed between *E. coli* and *B. subtilis*, suggesting that the mechanical properties of *E. coli* and *B. subtilis* are substantially similar.

Studies have found that the mechanical properties of bacterial cells appear to vary with the relative humidity.[52] Cell surfaces may undergo structural changes when they are dried in air. It should be noted that our antibacterial activity studies were conducted in aqueous solutions. To measure the mechanical properties of cell surfaces in an environment similar to the one in which they encounter SWCNTs, we carried the AFM studies in aqueous solution, all the cells were kept in 0.9 wt % NaCl solutions during the entire process of AFM imaging and force−distance curve measurements. As shown in Figure 6A,B, bacterial cells can be imaged in liquid with a reasonably good resolution. Figure 6C reveals the mechanical properties of different bacterial surfaces. The slopes of force−distance curves decrease in the following order: glass surface > *E. coli* > *P. aeruginosa* > *B. subtilis* > *S. aureus*. This indicates that the surfaces of gram-negative bacteria *E. coli* and *P. aeruginosa* are stiffer than those of gram-positive bacteria *B. subtilis* and *S. aureus*. In general, gram-negative bacteria are more resistant to antibiotics than gram-positive bacteria because gram-negative bacteria have a complex outer membrane, which, in part, excludes substances toxic to bacteria.[53] The complex outer membrane of gram-negative bacteria may have enhanced their surface stiffness. Stiffer bacterial surfaces have higher resistance to physical punctures by mobile nano darts, which would result in the lower bacterial death rates. These AFM results agree well with our antibacterial activity results.

Enhancing SWCNT Physical Punctures on Bacteria. We have demonstrated that the major cause of bacterial death is the physical puncture by SWCNTs. Along this line, enhancing the physical puncture (both frequency and intensity) on bacteria should be able to significantly improve SWCNT antibacterial activity. Individually dispersed SWCNTs are smaller in size compared to SWCNT aggregates, and they are more mobile in solution as well. Smaller size and higher mobility can enhance the SWCNT physical punctures on bacteria, leading to the observed superior antibacterial activity from individually dispersed SWCNT samples. This agrees well with previously published results[26] on MWCNTs: debundled, short, and dispersed MWCNTs demonstrated high antibacterial activities. Moreover, a recent study has reported that the antibacterial activity of SWCNT aggregates in saline solution is dependent on SWCNT concentration and treatment time.[28] We hypothesize that the chance of bacteria being punctured by SWCNTs is higher with the elevated SWCNT concentration and longer incubation time, which may result in higher cell death rates. As shown in Figure 7A, when the concentration of individually dispersed SWCNTs in Tween-20 saline solutions increases from 5 to 80 μg/mL, the death rate of *E. coli* increases from 58.8 ± 6.8% to 89.3 ± 2.7%. Small changes in the death rate were observed when SWCNT concentrations is above 80 μg/mL, which may be because most of the bacteria have already been killed at the 80 μg/mL of SWCNT concentration.

The dependence of SWCNT antibacterial activity on the SWCNT physical punctures on bacteria can be further demonstrated by changing the shaking speed during incubation. *E. coli* and *B. subtilis* were incubated for 2 h at various shaking speeds from 0 to 250 rpm in the presence of SWCNTs dispersed in Tween-20 solutions. Figure 7B shows that the death rates of both *E. coli* and *B. subtilis* increase with the increase of shaking speeds. A higher shaking speed remarkably enhances the mobility of both SWCNTs and bacteria in a solution, therefore leading to a higher frequency and intensity of collisions between SWCNTs and bacteria. We propose that more punctures on bacterial membranes result in greater chance of membrane damages, resulting in the increased cell death rates. The results in Figure 7 also strongly complement our suggestion that individu-

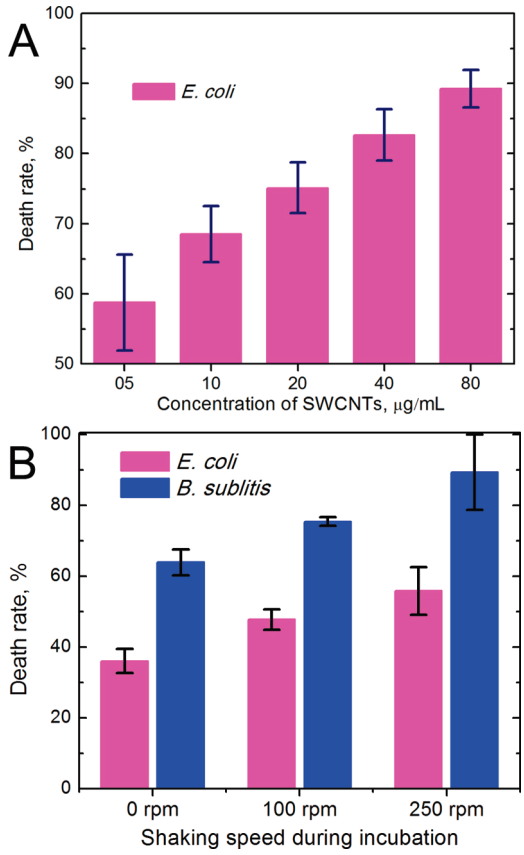

Figure 7. (A) Antibacterial activities of SWCNT at different concentrations: 10 mL of SWCNT (5−80 μg/mL dispersed in Tween-20 saline solutions) was incubated with 1 mL of *E. coli* dispersion (10^6−10^7 cfu/mL). (B) Antibacterial activities of SWCNTs (10 mL, 5 μg/mL) after 2 h incubation with *E. coli* and *B. subtilis* (1 mL, 10^6−10^7 cfu/mL) at different shaking speeds.

ally dispersed SWCNTs have a better antibacterial activity than SWCNT aggregates because individual SWCNTs are more mobile in the solution which enhances their physical punctures on bacteria.

CONCLUSION

Antibacterial activity of SWCNTs on various bacteria was investigated using pristine SWCNTs produced from Co-MCM-41 catalyst and purified by a centrifugation-based method. High-purity SWCNT samples helped to eliminate the possible contamination caused by impurities such as MWCNTs and amorphous and graphitic carbon nanoparticles. UV−vis−NIR absorption spectra confirmed the aggregation state can be regulated by dispersing SWCNTs in different solutions. Both the colony forming count method and the live/dead viability assay demonstrated that individually dispersed SWCNTs showed a higher antibacterial activity compared to SWCNT aggregates. SWCNT dispersions also exhibited higher antibacterial activity toward gram-positive bacteria (*B. subtilis* and *S. aureus*) than gram-negative bacteria (*E. coli* and *P. aeruginosa*). UV−vis absorption spectroscopy study at 260 nm and SEM images revealed that the bacterium death was related to the destruction of bacterial membrane. SWCNTs can be visualized as moving nano darts in a solution, attacking the bacteria, thereby degrading the bacterial cell integrity and causing the cell death. In this study, results also evidenced that inhibiting cell growth and oxidative stress were not the major reasons responsible for the SWCNT antibacterial activity. Co metal residues (up to 1 μg/mL) remaining on SWCNT samples had no detrimental effects on the antibacterial activity. AFM results obtained in aqueous solution showed that the mechanical properties of bacteria agreed with our antibacterial activity results, stiffer bacteria were more resistant against physical punctures by SWCNTs. Lastly, SWCNT antibacterial activity can be further improved by enhancing the SWCNT physical punctures on bacteria through individually dispersing SWCNTs, increasing SWCNT concentration, and elevating shaking speed during incubation.

MATERIALS AND METHODS

Synthesis and Purification of SWCNTs. Co-MCM-41 catalysts were synthesized following procedures described in previous publications.[54−56] Typically, 100 mg of catalysts were reduced at 500 °C under hydrogen first, and then carbon monoxide decomposition was carried out at 800 °C for SWCNT growth.[32−34] In this study, we used the centrifugation-based purification protocol developed early.[35] Briefly, MCM-41 silica supports were removed from as-synthesized SWCNTs by refluxing in 1 M NaOH twice. Without any further treatment, SWCNTs were suspended in 2 wt % SC (SigmaUltra) aqueous solution and sonicated using a cup-horn sonicator (SONICS, VCX-130) at 20 W for 30 min. After sonication, the suspension was centrifuged for 1 h at the force of 120000*g*. Subsequently, stable and semitransparent SWCNT supernatants were obtained. SWCNT supernatants were then filtered on filter membranes (25 nm mixed cellulose ester membrane, Millipore). After washing by deionized water, SWCNT solid powders were collected from the membranes. Further heating process was performed in a tube furnace under air at 350 °C for 30 min to remove adsorbed surfactant molecules from SWCNT surface.

Characterization of SWCNTs. Physical and chemical properties of SWCNT samples were characterized by various techniques including Raman spectroscopy, TGA, PLE, and UV−vis−NIR absorption spectroscopy, AFM, TEM, and SEM. Raman spectra were collected *via* a Renishaw Ramanscope in the backscattering configuration using 633 nm (1.96 eV) and 514 nm (2.41 eV) laser wavelengths over five random spots on SWCNT solid powers before dispersing them in solutions. TGA was performed with PerkinElmer Diamond TG/DTA Instruments. A SWCNT sample was placed in an alumina pan in the 200 sccm air flow. The sample was heated to 105 °C at a quick ramp and soaked at the temperature for 10 min to remove remaining moisture. Then the sample was heated up to 1025 °C at a 10 °C/min ramp. To correct the TGA profile, the process was repeated after the system was cooled to room temperature to collect data serving as the baseline. Photoluminescence excitation spectroscopy (PLE) measurement was performed on a Jobin-Yvon Nanolog-3 spectrofluorometer with an InGsAs detector. UV−vis−NIR absorption was conducted in the transmission mode on a Varian Cary 5000 UV−vis−NIR spectrophotometer using a 10 mm light path quartz cuvette. AFM measurement was conducted on a MFP3D

microscope (Asylum Research, Santa Barbara, CA) with a cantilever (Arrow NC, Nanoworld) in AC mode. A drop of SWCNT dispersion was dropcasted on a freshly cut mica surface followed by drying and rinsing of deionized water for AFM. TEM images of SWCNTs were taken by a Tecnai F20 200 kV microscope from Philips. SEM observations were carried out on a JEOL field-emission scanning electron microscope, model JSM-6700F.

Cell Preparation. Gram-negative bacteria *E. coli* (ATCC 25404), *P. aeruginosa* (ATCC 9027), and gram-positive bacteria *B. subtilis* (ATCC 6051), *S. aureus* (ATCC 6538) were chosen as the model organisms for antibacterial activity experiments. *E. coli, P. aeruginosa*, and *S. aureus* were grown in LB broth at 37 °C, and *B. subtilis* were grown at 30 °C. Cells were harvested in the mid-exponential growth phase. The cultures harvested in the mid-exponential growth phase were centrifuged at 6000 rpm for 10 min to pellet the cells, and the cell pellets were washed three times with saline solution to remove residual macromolecules and other growth medium constituents. The pellets were then resuspended in a saline solution. Bacterial suspensions were diluted to obtain cell samples containing 10^6-10^7 colony forming units (cfu/mL).

Measurements of Bacterial Activity. Antimicrobial activities of SWCNT samples have been investigated against *E. coli, P. aeruginosa*, *S. aureus*, and *B. subtilis*. Purified SWCNT solid samples (5 μg/mL) were first dispersed in saline solution (0.9 wt % NaCl), Tween-20 saline solution (0.1 wt % Tween-20 and 0.9 wt % NaCl), and SC solution (1 wt % SC) by sonication using a cup-horn sonicator (SONICS, VCX-130) at 20 W for 1 h. Clear SWCNT dispersions were obtained after sonication. A 10 mL portion of SWCNT dispersion (5 μg/mL) was incubated with 1 mL of bacterial suspensions (10^6-10^7 cfu/mL) for 2 h (at 0−250 rpm shaking speeds) at 37 or 30 °C, respectively. The antimicrobial evaluations were carried out by a colony forming count method and a live/dead viability assay (Invitrogen, USA). For the colony forming count method, 100 μL serial 10-fold dilutions with saline solution were spread onto LB plates and left to grow overnight at 37 or 30 °C. Colonies were counted and compared with control plates to calculate percentage growth inhibition. All treatments were prepared in duplicate and repeated on at least three separate occasions. Death rate % = (counts of control − counts of samples incubated with SWCNTs)/counts of control. The death rates obtained in the colony forming count method were further verified by the live/dead viability assay. Propidium iodide (PI) and SYTO 9 stock solutions from the assay kit were combined with an equal volume of *E. coli* or *B. subtilis* suspension. The mixtures were incubated at room temperature in the dark for 15 min and then observed under an epifluorescence microscope (Zeiss Axiovert 200). The death rate of bacteria was taken as the number of bacteria stained with PI (dead bacteria) divided by the number of bacteria stained with PI plus SYTO 9 (total bacteria).

Integrity of Cell Membranes. Bacterial cell membrane integrity was examined by UV spectroscopy at 260 nm. If the bacteria membrane is disrupted, release of cell cytoplasmic constituents can be surveiled. The amount of DNA and RNA released from the cytoplasm can be estimated by the detection of absorbance at 260 nm.[44] After 2 h incubation with 5 μg/mL SWCNTs, the bacterial suspensions were then immediately filtered with 0.22 μm syringe filters to remove the bacteria. The supernatant was then diluted appropriately, and optical density at 260 nm was recorded.

Cell Morphology Observation. The morphological changes of *E. coli, P. aeruginosa*, *S. aureus,* and *B. subtilis* were investigated by SEM. Bacterial suspensions were condensed by centrifugation at 6000 rpm, 4 °C, and quickly fixed with 2% glutaraldehyde and 1% osmium tetroxide. Then the cells were dehydrated with sequential treatment with 30, 50, 70, 80, 90, and 100% ethanol for 15 min; 10 μL of dehydrated cells were dropped on a glass slide to dry at room temperature. The dried samples were sputter-coated with gold for SEM.

OD Growth. For OD growth curve measurements, 100 μL of *E. coli* or *B. subtilis* (10^8-10^9 cfu/mL) were mixed with 900 μL of LB broth or Tween-20 saline solutions (0.1 wt % Tween-20 and 0.9 wt % NaCl). Cell samples were then incubated at 37 or 30 °C in 24-well cell culture plates. Cell growth was monitored by measuring the OD at 600 nm every hour on a Benchmark Plus microplate spectrophotometer. The growth curves were obtained by plotting OD values *vs* growth time.

Impact of Bacteriostatic Agent. Sulfadiazine was dissolved in a mixture of methanol and acetone (1:1) at 10 mg/mL;[57] 50 μg of sulfadiazine (5 μL of the 10 mg/mL solution) was added into the mixture of 1 mL bacterial suspensions (*E. coli* or *B. subtilis*, 10^6-10^7 cfu/mL) and 10 mL SWCNT dispersion (5 μg/mL). The bacterial suspensions were then incubated for 2 h at 37 or 30 °C. In control experiments, 50 μg of sulfadiazine was added into 1 mL of bacterial suspensions (*E. coli* or *B. subtilis*, 10^6 to 10^7 cfu/mL) and 10 mL of Tween-20 saline solutions without the presence of SWCNTs. The antimicrobial death rates were determined by the colony forming count method.

Oxidation−Reduction Potential of SWCNT Dispersions. The ORP of SWCNT dispersions were measured using an ORP tester (Oakton Instruments, ORPTestr 10). Each tested sample was purged with nitrogen for 15 min prior to reading. SWCNT dispersions at various concentrations in saline solutions (0.9 wt % NaCl) and the Tween-20 saline solutions (0.1 wt % Tween-20 and 0.9 wt % NaCl) were measured 3−5 times to obtain the standard deviation.

Monitoring Oxidation of Cellular Components. A Thiol and Sulfide Quantitation Kit (Molecular Probes, Invitrogen) was used to measure the level of thiols in proteins. Two sets of assays were performed to assess the SWCNT oxidation of proteins both in and out of cell membranes. For cytoplasmic proteins, 10 mL of SWCNT dispersions (5 μg/mL in the Tween-20 saline solution) were incubated with 1 mL of *E. coli* or *B. subtilis* (10^6-10^7 cfu/mL) suspensions for 2 h at 37 or 30 °C. The mixtures were centrifuged at 6000 rpm for 10 min to pellet the cells, and the cell pellets were washed three times with saline solutions. The cell pellets were then resuspended in saline solutions. In a glovebox (SYS1−2GB, Innovative Technology), cells are lysed by sonication (SONICS, VCX-130) at 20 W for 1 min. Supernatants obtained after centrifugation were transferred to fresh tubes. About 2.5 μg of proteins were used for each Thiol assay. The protein concentrations in cell extracts were determined by a Pierce BCA protein assay kit. For cell-free assays, SWCNT dispersions (5 μg /mL) were incubated with bovine serum albumin (BSA) solutions (diluted from 2 mg/mL concentrated solutions by Bio-Rad Quick Start, 1 thiol group per protein, total 3 μg of proteins). For each assay, a negative control was incubated with Tween-20 saline solutions and a positive control was incubated with 5 mM *tert*-butylhydroperoxide in Tween-20 saline solutions. All solutions used for thiol determination were degassed in a vacuum oven <1 Torr (DZF-6053, Shanghai Yiheng Instruments). The thiol assays were conducted in a microplate format as described in the kit manufacturer's protocol. The thiol concentration in samples was shown in nmols.

Mechanical Properties of Bacterial Membranes. *E. coli, P. aeruginosa*, *S. aureus*, and *B. subtilis* were studied by AFM in saline solution (0.9 wt % NaCl). Glass slides were chosen as substrates and cleaned with alcohol, acetone, and deionized water; 10 μL of poly(L-lysine) solution was dropped in the middle of clean glass sides and dried in room temperature to facilitate the immobilization of cells on the glass surface.[58] The harvested bacteria were washed with saline solutions as described previously. Bacterial suspensions (50 μL) were drop-casted on a treated glass slide and allowed to sit for 20 min to allow cells to anchor on the surface.[58] AFM images were conducted on the MFP3D microscope in contact mode using Silicon probes (ContAl-G from Budget Sensors, tip radius <10 nm). The position and shape of the bacteria were first identified on AFM images. To acquire force−distance curves, the sensitivity calibration of AFM probes was performed first before force measurement. At least 10 random locations on the same bacteria were selected to record the force−distance curves. The force curves were obtained with a constant tip approach velocity of 200 nm/s, and AFM tips were pressed against bacteria until the force reached the set point of 3 nN. For AFM imaging in a dry environment, 10 μL of washed bacterial suspension were dropped onto clean glass slides and air dried at room temperature. AFM images were conducted in tapping mode using Silicon probes (NCH from Nano World).

Acknowledgment. This work was supported by Environment & Water Industry Development Council, Singapore (0802-IRIS-12) and National Research Foundation, Singapore (NRF-CRP2-2007-02). We appreciate helpful discussion with Mary B. Chan-Park, Vincent Chan, and Rongrong Jiang from Nanyang Technological University. The authors thank reviewers for helpful comments to improve this work.

Supporting Information Available: Characterization of SWCNT samples using various techniques including Raman spectroscopy, TGA, PLE, AFM, SEM and TEM; releasing of 260 nm absorbing materials from bacteria after incubating with SWCNT dispersions; OD growth curves of *E. coli* and *B. subtilis* in LB broth and the Tween-20 saline solution, and the impact of a bacterial static agent on the bacterial death rate; releasing of 260 nm absorbing materials from bacteria after incubating with SWCNTs obtained after centrifugation at different forces; AFM images of air-dried *E. coli* and *B. subtilis* and typical force−distance curves obtained on glass surface, *E. coli*, and *B. subtilis* in air. This material is available free of charge *via* the Internet at http://pubs.acs.org.

REFERENCES AND NOTES

1. Iijima, S. Helical Microtubules of Graphitic Carbon. *Nature* **1991**, *354*, 56–58.
2. Jorio, A.; Dresselhaus, G.; Dresselhaus, M. S., In *Carbon Nanotubes, Advanced Topics in the Synthesis, Structure, Properties and Applications*; Springer: Berlin, 2008; pp 1−12.
3. Lu, F. S.; Gu, L. R.; Meziani, M. J.; Wang, X.; Luo, P. G.; Veca, L. M.; Cao, L.; Sun, Y. P. Advances in Bioapplications of Carbon Nanotubes. *Adv. Mater.* **2009**, *21*, 139–152.
4. Kang, S.; Pinault, M.; Pfefferle, L. D.; Elimelech, M. Single-Walled Carbon Nanotubes Exhibit Strong Antimicrobial Activity. *Langmuir* **2007**, *23*, 8670–8673.
5. Mauter, M. S.; Elimelech, M. Environmental Applications of Carbon-Based Nanomaterials. *Environ. Sci. Technol.* **2008**, *42*, 5843–5859.
6. Brady-Estevez, A. S.; Kang, S.; Elimelech, M. A Single-Walled-Carbon-Nanotube Filter for Removal of Viral and Bacterial Pathogens. *Small* **2008**, *4*, 481–484.
7. Yuan, W.; Jiang, G. H.; Che, J. F.; Qi, X. B.; Xu, R.; Chang, M. W.; Chen, Y.; Lim, S. Y.; Dai, J.; Chan-Park, M. B. Deposition of Silver Nanoparticles on Multiwalled Carbon Nanotubes Grafted with Hyperbranched Poly(amidoamine) and Their Antimicrobial Effects. *J. Phys. Chem. C* **2008**, *112*, 18754–18759.
8. Shen, M. W.; Wang, S. H.; Shi, X. Y.; Chen, X. S.; Huang, Q. G.; Petersen, E. J.; Pinto, R. A.; Baker, J. R.; Weber, W. J. Polyethyleneimine-Mediated Functionalization of Multiwalled Carbon Nanotubes: Synthesis, Characterization, and *In Vitro* Toxicity Assay. *J. Phys. Chem. C* **2009**, *113*, 3150–3156.
9. Nepal, D.; Balasubramanian, S.; Simonian, A. L.; Davis, V. A. Strong Antimicrobial Coatings: Single-Walled Carbon Nanotubes Armored with Biopolymers. *Nano Lett.* **2008**, *8*, 1896–1901.
10. Kulinowski, K. M.; Colvin, V. L. The Environmental Impact of Engineered Nanomaterials. *ACS Symp. Ser.* **2005**, *890*, 21–26.
11. Christian, P.; Von der Kammer, F.; Baalousha, M.; Hofmann, T. Nanoparticles: Structure, Properties, Preparation and Behaviour in Environmental Media. *Ecotoxicology* **2008**, *17*, 326–343.
12. Klaine, S. J.; Alvarez, P. J. J.; Batley, G. E.; Fernandes, T. F.; Handy, R. D.; Lyon, D. Y.; Mahendra, S.; McLaughlin, M. J.; Lead, J. R. Nanomaterials in the Environment: Behavior, Fate, Bioavailability, and Effects. *Environ. Toxicol. Chem.* **2008**, *27*, 1825–1851.
13. Hochella, M. F.; Lower, S. K.; Maurice, P. A.; Penn, R. L.; Sahai, N.; Sparks, D. L.; Twining, B. S. Nanominerals, Mineral Nanoparticles, and Earth Systems. *Science* **2008**, *319*, 1631–1635.
14. Hurt, R. H.; Monthioux, M.; Kane, A. Toxicology of Carbon Nanomaterials: Status, Trends, and Perspectives on the Special Issue. *Carbon* **2006**, *44*, 1028–1033.
15. Guo, L.; Morris, D. G.; Liu, X. Y.; Vaslet, C.; Hurt, R. H.; Kane, A. B. Iron Bioavailability and Redox Activity in Diverse Carbon Nanotube Samples. *Chem. Mater.* **2007**, *19*, 3472–3478.
16. Pulskamp, K.; Diabate, S.; Krug, H. F. Carbon Nanotubes Show No Sign of Acute Toxicity but Induce Intracellular Reactive Oxygen Species in Dependence on Contaminants. *Toxicol. Lett.* **2007**, *168*, 58–74.
17. Li, Q. L.; Mahendra, S.; Lyon, D. Y.; Brunet, L.; Liga, M. V.; Li, D.; Alvarez, P. J. J. Antimicrobial Nanomaterials for Water Disinfection and Microbial Control: Potential Applications and Implications. *Water Res.* **2008**, *42*, 4591–4602.
18. Narayan, R. J.; Berry, C. J.; Brigmon, R. L. Structural and Biological Properties of Carbon Nanotube Composite Films. *Mater. Sci. Eng., B* **2005**, *B123*, 123–129.
19. Liu, Z.; Sun, X. M.; Nakayama-Ratchford, N.; Dai, H. J. Supramolecular Chemistry on Water-Soluble Carbon Nanotubes for Drug Loading and Delivery. *ACS Nano* **2007**, *1*, 50–56.
20. Chen, X.; Tam, U. C.; Czlapinski, J. L.; Lee, G. S.; Rabuka, D.; Zettl, A.; Bertozzi, C. R. Interfacing Carbon Nanotubes with Living Cells. *J. Am. Chem. Soc.* **2006**, *128*, 6292–6293.
21. Cherukuri, P.; Bachilo, S. M.; Litovsky, S. H.; Weisman, R. B. Near-Infrared Fluorescence Microscopy of Single-Walled Carbon Nanotubes in Phagocytic Cells. *J. Am. Chem. Soc.* **2004**, *126*, 15638–15639.
22. Dumortier, H.; Lacotte, S.; Pastorin, G.; Marega, R.; Wu, W.; Bonifazi, D.; Briand, J. P.; Prato, M.; Muller, S.; Bianco, A. Functionalized Carbon Nanotubes Are Non-Cytotoxic and Preserve the Functionality of Primary Immune Cells. *Nano Lett.* **2006**, *6*, 1522–1528.
23. Kam, N. W. S.; O'Connell, M.; Wisdom, J. A.; Dai, H. J. Carbon Nanotubes As Multifunctional Biological Transporters and near-Infrared Agents for Selective Cancer Cell Destruction. *Proc. Nat. Acad. Sci. U.S.A.* **2005**, *102*, 11600–11605.
24. Liu, Z.; Tabakman, S.; Welsher, K.; Dai, H. J. Carbon Nanotubes in Biology and Medicine: *In Vitro* and *in Vivo* Detection, Imaging, and Drug Delivery. *Nano Res.* **2009**, *2*, 85–120.
25. Kang, S.; Herzberg, M.; Rodrigues, D. F.; Elimelech, M. Antibacterial Effects of Carbon Nanotubes: Size Does Matter. *Langmuir* **2008**, *24*, 6409–6413.
26. Kang, S.; Mauter, M. S.; Elimelech, M. Physicochemical Determinants of Multiwalled Carbon Nanotube Bacterial Cytotoxicity. *Environ. Sci. Technol.* **2008**, *42*, 7528–7534.
27. Kang, S.; Mauter, M. S.; Elimelech, M. Microbial Cytotoxicity of Carbon-Based Nanomaterials: Implications for River Water and Wastewater Effluent. *Environ. Sci. Technol.* **2009**, *43*, 2648–2653.
28. Arias, L. R.; Yang, L. J. Inactivation of Bacterial Pathogens by Carbon Nanotubes in Suspensions. *Langmuir* **2009**, *25*, 3003–3012.
29. Wick, P.; Manser, P.; Limbach, L. K.; Dettlaff-Weglikowska, U.; Krumeich, F.; Roth, S.; Stark, W. J.; Bruinink, A. The Degree and Kind of Agglomeration Affect Carbon Nanotube Cytotoxicity. *Toxicol. Lett.* **2007**, *168*, 121–131.
30. Saleh, N. B.; Pfefferle, L. D.; Elimelech, M. Aggregation Kinetics of Multiwalled Carbon Nanotubes in Aquatic Systems: Measurements and Environmental Implications. *Environ. Sci. Technol.* **2008**, *42*, 7963–7969.
31. Liu, X. Y.; Gurel, V.; Morris, D.; Murray, D. W.; Zhitkovich, A.; Kane, A. B.; Hurt, R. H. Bioavailability of Nickel in Single-Wall Carbon Nanotubes. *Adv. Mater.* **2007**, *19*, 2790–2796.
32. Ciuparu, D.; Chen, Y.; Lim, S.; Haller, G. L.; Pfefferle, L. Uniform-Diameter Single-Walled Carbon Nanotubes Catalytically Grown in Cobalt-Incorporated MCM-41. *J. Phys. Chem. B* **2004**, *108*, 503–507.
33. Chen, Y.; Ciuparu, D.; Lim, S.; Yang, Y.; Haller, G. L.; Pfefferle, L. Synthesis of Uniform Diameter Single-Wall Carbon Nanotubes in Co-MCM-41: Effects of the Catalyst

Prereduction and Nanotube Growth Temperatures. *J. Catal.* **2004**, *225*, 453–465.
34. Chen, Y.; Ciuparu, D.; Lim, S.; Yang, Y.; Haller, G. L.; Pfefferle, L. Synthesis of Uniform Diameter Single Wall Carbon Nanotubes in Co-MCM-41: Effects of CO Pressure and Reaction Time. *J. Catal.* **2004**, *226*, 351–362.
35. Wei, L.; Wang, B.; Wang, Q.; Li, L. J.; Yang, Y. H.; Chen, Y. Effect of Centrifugation on the Purity of Single-Walled Carbon Nanotubes from MCM-41 Containing Cobalt. *J. Phys. Chem. C* **2008**, *112*, 17567–17575.
36. Itkis, M. E.; Perea, D. E.; Niyogi, S.; Rickard, S. M.; Hamon, M. A.; Hu, H.; Zhao, B.; Haddon, R. C. Purity Evaluation of As-Prepared Single-Walled Carbon Nanotube Soot by Use of Solution-Phase Near-IR Spectroscopy. *Nano Lett.* **2003**, *3*, 309–314.
37. Moore, V. C.; Strano, M. S.; Haroz, E. H.; Hauge, R. H.; Smalley, R. E.; Schmidt, J.; Talmon, Y. Individually Suspended Single-Walled Carbon Nanotubes in Various Surfactants. *Nano Lett.* **2003**, *3*, 1379–1382.
38. Wenseleers, W.; Vlasov, I. I.; Goovaerts, E.; Obraztsova, E. D.; Lobach, A. S.; Bouwen, A. Efficient Isolation and Solubilization of Pristine Single-Walled Nanotubes in Bile Salt Micelles. *Adv. Funct. Mater.* **2004**, *14*, 1105–1112.
39. Elgrabli, D.; Abella-Gallart, S.; Aguerre-Chariol, O.; Robidel, F.; Rogerieux, F.; Boczkowski, J.; Lacroix, G. Effect of BSA on Carbon Nanotube Dispersion for *in Vivo* and *in Vitro* Studies. *Nanotoxicology* **2007**, *1*, 266–278.
40. Rastogi, R.; Kaushal, R.; Tripathi, S. K.; Sharma, A. L.; Kaur, I.; Bharadwaj, L. M. Comparative Study of Carbon Nanotube Dispersion using Surfactants. *J. Colloid Interface Sci.* **2008**, *328*, 421–428.
41. Dong, L.; Joseph, K. L.; Witkowski, C. M.; Craig, M. M. Cytotoxicity of Single-Walled Carbon Nanotubes Suspended in Various Surfactants. *Nanotechnology* **2008**, 19.
42. Schubert, R.; Beyer, K.; Wolburg, H.; Schmidt, K. H. Structural-Changes in Membranes of Large Unilamellar Vesicles After Binding of Sodium Cholate. *Biochemistry* **1986**, *25*, 5263–5269.
43. Treyer, M.; Walde, P.; Oberholzer, T. Permeability Enhancement of Lipid Vesicles to Nucleotides by Use of Sodium Cholate: Basic Studies and Application to an Enzyme-Catalyzed Reaction Occurring Inside the Vesicles. *Langmuir* **2002**, *18*, 1043–1050.
44. Chen, C. Z. S.; Cooper, S. L. Interactions between Dendrimer Biocides and Bacterial Membranes. *Biomaterials* **2002**, *23*, 3359–3368.
45. Strauss, E.; Dingle, J. H.; Finland, M. Studies on the Mechanism of Sulfonamide Bacteriostasis, Inhibition and Resistance—Experiments with *E. coli* in a Synthetic Medium. *J. Immunol.* **1941**, *42*, 313–329.
46. Strauss, E.; Dingle, J. H.; Finland, M. Studies on the Mechanism of Sulfonamide Bacteriostasis, Inhibition and Resistance—Experiments with *Staphylococcus aureus*. *J. Immunol.* **1941**, *42*, 331–342.
47. Erin, E.; Connor, M. Sulfonamide Antibiotics. *Prim. Care Update Ob/Gyns* **1998**, *5*, 32–35.
48. Lyon, D. Y.; Alvarez, P. J. J. Fullerene Water Suspension (*n*C(60)) Exerts Antibacterial Effects *via* ROS-Independent Protein Oxidation. *Environ. Sci. Technol.* **2008**, *42*, 8127–8132.
49. Lyon, D. Y.; Brunet, L.; Hinkal, G. W.; Wiesner, M. R.; Alvarez, P. J. J. Antibacterial Activity of Fullerene Water Suspensions (*n*C(60)) Is Not Due to ROS-Mediated Damage. *Nano Lett.* **2008**, *8*, 1539–1543.
50. Heinz, W. F.; Hoh, J. H. Spatially Resolved Force Spectroscopy of Biological Surfaces Using the Atomic Force Microscope. *Trends Biotechnol.* **1999**, *17*, 143–150.
51. Carl, P.; Schillers, H. Elasticity Measurement of Living Cells with an Atomic Force Microscope: Data Acquisition and Processing. *Pfluegers Arch.* **2008**, *457*, 551–559.
52. Thwaites, J. J.; Surana, U. C. Mechanical Properties of *Bacillus subtilis* Cell Walls—Effects of Removing Residual Culture Medium. *J. Bacteriol.* **1991**, *173*, 197–203.
53. Voet, D.; Voet, J. G.; Pratt, C. W., *Fundamentals of Biochemistry;* John Wiley & Sons, Inc.: New York, 2006.
54. Lim, S.; Ciuparu, D.; Chen, Y.; Yang, Y.; Pfefferle, L.; Haller, G. L. Pore Curvature Effect on the Stability of Co-MCM-41 and the Formation of Size-Controllable Subnanometer Co Clusters. *J. Phys. Chem. B* **2005**, *109*, 2285–2294.
55. Chen, Y.; Ciuparu, D.; Lim, S.; Haller, G. L.; Pfefferle, L. D. The Effect of the Cobalt Loading on the Growth of Single Wall Carbon Nanotubes by CO Disproportionation on Co-MCM-41 Catalysts. *Carbon* **2006**, *44*, 67–78.
56. Lim, S.; Yang, Y.; Ciuparu, D.; Wang, C.; Chen, Y.; Pfefferle, L.; Haller, G. L. The Effect of Synthesis Solution pH on the Physicochemical Properties of Co Substituted MCM-41. *Top. Catal.* **2005**, *34*, 31–40.
57. Meneceur, P.; Bouldouyre, M. A.; Aubert, D.; Villena, I.; Menotti, J.; Sauvage, V.; Garin, J. F.; Derouin, F. *In Vitro* Susceptibility of Various Genotypic Strains of Toxoplasma Gondii to Pyrimethamine, Sulfadiazine, and Atovaquone. *Antimicrob. Agents Chemother.* **2008**, *52*, 1269–1277.
58. Giesbrecht, P.; Kersten, T.; Wecke, J. Fan-Shaped Ejections of Regularly Arranged Murosomes Involved in Penicillin-Induced Death of Staphylococci. *J. Bacteriol.* **1992**, *174*, 2241–2252.